

The role of material properties for the mechanical adaptation at branch junctions

Karin Jungnikl · Jürgen Goebbels ·
Ingo Burgert · Peter Fratzl

Received: 12 December 2007 / Revised: 5 November 2008 / Accepted: 3 December 2008 / Published online: 24 December 2008
© The Author(s) 2008. This article is published with open access at Springerlink.com

Abstract Branch junctions are mechanically particularly interesting areas of trees, because they have to withstand a combination of static and dynamic loads, from the stem as well as from the branch. In the present work, the local adaptation of material properties at branch junctions was assessed by mapping microfibril angle and tissue density. Images of the density distribution were obtained by computer tomography (CT). Wide angle X-ray scattering (WAXS) was used to determine the microfibril angle distribution with high-resolution around the junctions. The stem tissue around the junctions showed increased density and microfibril angle, which points towards an optimisation for fracture toughness. The tissue at the branch bases showed low density combined with high MFA, which provides deformability and flexibility and might act as protection of the stem against load transmission from the branch.

Keywords Branch junction · Computer tomography (CT) · Microfibril angle (MFA) · Notch stresses · Wide angle X-ray scattering (WAXS)

Introduction

Branch junctions are structures that withstand strong static and dynamic loads for many years. The mechanical design of a branch junction has to provide not only the stability and optimal functionality of the branch but also mechanical safety for the stem. Another important property is damage tolerance when the branch is broken or shed, e.g. defence against micro-organisms at the defect (Shigo 1989). To the tree, the mechanical safety of the stem is of primary concern and has to be balanced versus the mechanical stability of the branches. They are, on the one hand, necessary for photosynthesis but, on the other hand, increase the sail area, creating a potential source of danger to the stem in the case of strong wind. From the fracture mechanical perspective, a branch junction also represents a notch in the stem. Stem failure often occurs at damaged branch junctions or knots. It was shown that force controlled optimisation of the shape of stem and branches is an essential tool for the control of the stress distribution at the surface (Mattheck 1998) and also for introducing preferred points of failure as safety mechanism or for propagation purposes (Niklas and Spatz 2000; Beismann et al. 1997). A local change of the branch diameter at the branch collar (Shigo 1989) or at a crotch (Genenz et al. 1997) were described as such ‘preferred points of failure’.

The alternating pattern of interlocking stem- and branch bound tissue below the branch is an important feature that provides stability for the junction. Its mechanical implications were discussed in detail by Shigo (1989). The stem bound tissue stabilises the branch collar and the large surface area between the growth ring layers increases the fracture toughness (Fig. 1).

A study by electronic speckle pattern interferometry (ESPI) (Müller et al. 2006) provided a direct picture of the

Communicated by T. Speck.

K. Jungnikl (✉) · I. Burgert · P. Fratzl
Department of Biomaterials, Max Planck Institute of Colloids and Interfaces, Research Campus Golm, Potsdam, Germany
e-mail: karin.jungnikl@mpikg.mpg.de

J. Goebbels
Federal Institute for Materials Research and Testing (BAM),
Lichterfelde, Berlin, Germany

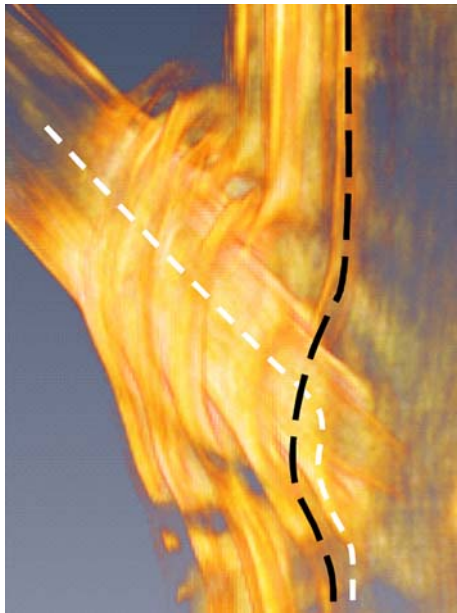


Fig. 1 The alternating pattern of stem- (black) and branch bound (white) tissue below the branch. Section of the CT taken of junction I (left branch in Fig. 2). The dense latewood layers appear bright

strain field in a longitudinal cross section of a junction. A comparison was made between the strain field in a branch junction and polyester cast of the same shape. The branch junction showed a homogeneous strain distribution within the stem while strain concentrations were observed in the polyester cast. The homogeneous strain distribution in the wood sample implied a situation where ‘*stress is high in zones of high modulus and low in zones of low modulus*’ (Müller et al. 2006). From the results, it was concluded that the distribution of the material properties should be adapted locally. The aim of the present work was to show this adaptation directly, by measuring the local distribution of material properties.

At each growth increment, the mechanical properties of the newly formed wood tissue are adapted to the local mechanical demands. Microfibril angle (MFA) and tissue density have been shown to determine the stiffness and fracture behaviour of softwood (Cave 1969; Reiterer et al. 1999). The MFA has been shown to have a direct influence on energy absorption and tensile stiffness (Reiterer et al. 2001). It is known to be adapted in the course of diameter growth from pith to bark and along the length of stem and branches (Lichtenegger et al. 1998; Färber et al. 2001). The direct influence of the tissue density on material strength and stiffness is e.g. visible in the mechanical properties of latewood (LW) and earlywood (EW) with similar MFA. In the present study, the contribution of the material properties to the mechanical stability of branch junctions was described by the local distribution of microfibril angle and tissue density.

Materials and methods

Material

The samples were collected from three young pine trees grown on a north facing slope in Waldviertel/Austria at around 900 m altitude. All trees grew at the edge of a forest and were exposed to high snow loads during winter. Two of them (*Tree I* and *II*) grew closer to the edge than the third (*Tree III*) which was taken from a more protected site in a clearing a few meters inwards the forest. Trees *I* and *III* contained compression wood in the stem. The examined branch junctions were selected at a height of the trees where the branches were alive, the stem/branch diameter ratio comparable and the diameters high enough to suggest that the branch would produce significant loads on the stem. The diameters of branch and stem (without bark) were for branch *I* 18 and 50 mm, resulting in a diameter ratio of 0.35, for branch *II* 16 and 40 mm (0.40) and for branch *III* 14 and 45 mm (0.31). The number of growth rings in the stem above the branch was six (*Tree II*) and seven (*Trees I* and *III*). The angle between stem and branches was 45° directly at the stem for all samples but changed after a couple of centimeter where the branches started bending. The selected junctions were facing the forest, pointing uphill, where no compression wood was formed in the stem. All branches were bent at a couple of cm distally from the stem. Branch *I* was bent sideways by the (west)wind, kept more or less the initial 45° angle with the stem throughout the length of the branch and had a pronounced branch collar. Branch *II* and *III* were bent to an almost horizontal position and had less pronounced collars, probably rather to be termed as stem collars (Shigo 1989). The observed shape and pronouncedness of the collars correspond well with the classification by vitality (due to shading) described by Mattheck (1998).

Computer tomography (CT)

A CT was made of branch junction *I* at the Federal Institute for Materials Research and Testing (BAM) Berlin/Lichterfelde with a high-resolution 3D-computer tomograph equipped with a 225 kV microfocus X-ray generator and a 2D amorphous Silicon detector (2048 × 2048 pixel à 200 × 200 μm²). The CT was measured using a 2 mm Al-filter at 60 kV/267 μA. The sample was rotated 360° at 900 steps and 10 s exposures per step and scanned at 0.17 × 0.17 × 0.17 mm voxel size. The size of the reconstructed picture was (1,023 × 1,023 × 845 pixel). The greyscale represents the X-ray absorption of the material at the respective sample position (bright areas for high absorption, dark areas for low absorption, see e.g. Fig. 2). The density variation of the cell wall material itself

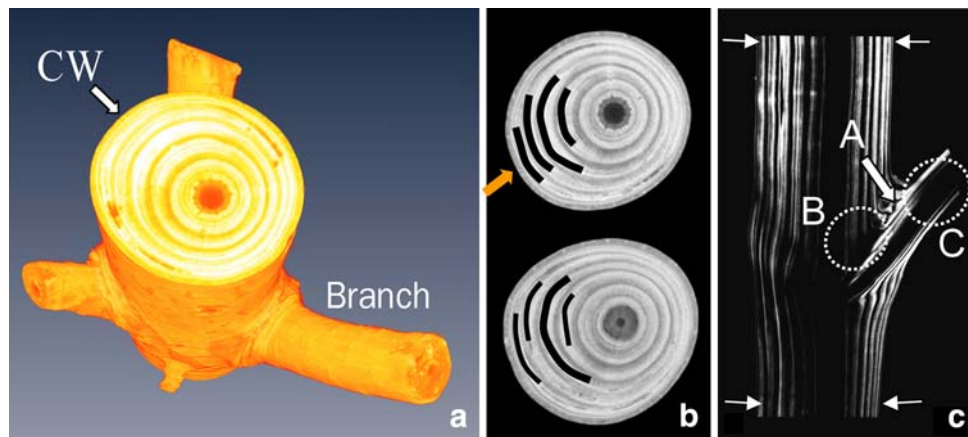


Fig. 2 CT of junction I **a** 3D view branch whorl carrying three branches and some rudimentary twigs. Areas with high density appear bright. *Arrow* pronounced compression wood (CW) opposite the examined junction. **b** Stem cross section above and below the junction, CW tissue with higher density (*arrow*) is highlighted with *black lines*. At the underside, the increased density and growth ring width is partially related to the other branches. Above the branch, the increased density is due to compression wood and a slight rotation in

the course of the years can be seen. **c** The branch is embedded at an angle of 45°. *Arrow* “A” indicates the spatial restriction of the high density branch LW, encircled areas “B” and “C” indicate areas of low density at the branch base (see also Fig. 1) and inside the stem. The *small arrows* indicate the approximate positions of the sections in **b**. In **b** and **c**, the *greyscale* threshold of the reconstructed picture was adjusted to show the density gradient only within the latewood. Areas with low density (pith, earlywood) appear *black*

is very small, the variation of the absorption in the sample was therefore directly related to the relative cell wall fraction. An exception may be the material directly at the junction where the tissue is known to have a different cell wall composition and to include additional compounds like lignans and resins that might influence the density.

Microfibril angle (MFA) measurements

Samples were taken from the stem at two or three distances both above and below the junction (~1 cm distance between the positions) and with higher resolution directly at the junction. For the samples taken further away from the junction (stem tissue), MFAs were determined for the three outermost growth rings at each position. For the samples taken directly at the junction, this was possible for the majority of the positions, at some positions only two growth rings were accessible. For sample ‘*Tree I*’ the MFA was mapped around the junction. For tree *II* and *III*, MFA measurements were made at four positions directly at the left and the right side of the branch collar.

The samples from the stem tissue were cut into tangential (LT) slices of 20–50 μm thickness parallel to the fibre direction using a microtome. For the samples taken from the interface tissue directly at the branch junction, the sections were cut with a razor blade and the thickness was around 200 μm. Wide angle scattering (WAXS) patterns were collected at a sample-detector distance of 5 cm using CuK α radiation (wavelength 1.54 Å) selected by a bent multilayer. A Nanostar instrument (Bruker AXS Karlsruhe) was used and the patterns were collected with

a 2D position sensitive detector. The MFA was calculated from the 020 reflection according to the method described by Lichtenegger et al. (1998). The calculated value represents an average MFA in the sample section hit by the beam.

Results and discussion

The three samples provided the opportunity to observe the tissue adaptation in very different situations. The junctions II and III showed an even MFA distribution in the expected range of normal softwood (i.e. low MFA) in the stem and also beside the branch, while junction I showed a pronounced horizontal asymmetry, in MFA as well as in density distribution. Figure 2 shows the CT taken from junction I. The brightness indicates areas of higher and lower tissue density. The growth rings, the compression wood region in the stem tissue and the density variation around the branch junction are clearly distinguishable. The density of the LW-layers in the branch and in the stem is increased at the intersection (Fig. 2c). The increase of density of the LW-tissue in the branch is restricted to the junction and the density decreases rapidly a couple of cm distally from the stem. The tissue in the core of the branch also shows a low density (comparable to the density of pith and EW-tissue in the stem) and no pronounced density gradient between earlywood and latewood. The density of pith and juvenile wood in the stem is considerably lower than in the outer growth rings. An area of lower density is also visible above the branch junction.

An angle of 45° at the junction of the branch was found in all three samples, but only branch I maintained this angle throughout its length. Besides (depending on the site) possible advantages for accessing sunlight, mechanical advantages of an angle significantly smaller than 90° are a reduced momentum at the junction, even more important when dynamic wind loads are applied, and reduced shear in the branch. An angle of 45° also results in an even distribution of the axial static load from the branch weight that is transferred to the stem (Böge 2006). A second feature of junction I that points to a stronger adaptation to wind loads than in the other samples is the pronounced branch collar [‘preferred point of failure’ (Niklas and Spatz 2000; Shigo 1989)].

A sketch of the latewood MFA distribution is given in Fig. 3 (the values in the figure are averages of all measurements at the respective position). Earlywood MFAs were also measured for junction I, but the pattern around the junction differed strongly between the growth rings. Water transport probably plays a dominant role in the mechanical adaptation of earlywood tissue; the influence of the external loads was therefore difficult to assess and only the latewood MFA were considered in the figures and in the discussion.

In the stem tissue of junction II and III, the MFA ranged from 7 to 20° . The values in the tissue directly above and below the junction increased to around 30° . In the tissue beside the branch, the MFA values were in the range of the stem tissue further away (10 – 13°). Junction I showed a pronounced horizontal asymmetry, with the highest MFA in the latewood of the outermost growth ring at the west facing (windward) side of the junction (34 – 47°). The MFA in the stem latewood was partially in the range of the stem

compression wood on the opposite side of the stem (average of 18 compression wood measurements was $\sim 40^\circ$). While in junction II and III the MFA was lower above the branch than below, this situation was reverse in junction I. Junction II and III further showed a significant increase of the MFA in the stem tissue directly above and below the junction, while such an increase was not so pronounced in junction I. MFA measurements for the branch of junction I revealed MFAs of 40 – 50° at the branch base, in the branch tissue inside the stem and at the underside of the branch and MFAs of 38 – 39° at the upper side outside the stem.

The primary mechanical demand on the outer LW-layers of a stem is the uptake of tensile forces; as a consequence, the primary concern of shape adaptation at a knot was described to be the optimisation of the flow of the axial tensile forces around the ‘notch’ (Mattheck 1998). Tissue with low MFA is particularly stiff and, thus, designed to resist axial tensile forces. The formation of stem collar tissue with low MFA beside the branches II and III can therefore be interpreted as an additional adaptation mechanism to optimise the tissue for the abovementioned function.

Branch junction I showed a different situation, with several features that can be interpreted as adaptation mechanisms to dynamic loads from the west wind (the main wind direction in this region) and high snow loads in winter. A combination of shape- and material adaptation to control the stress distribution was observable (Fig. 4). This sample showed nicely the interaction of three biomechanical adaptation factors—the radius of stem and branch (adapted by amount of tissue growth), tissue density (cell wall thickness) and MFA. The observation that swaying

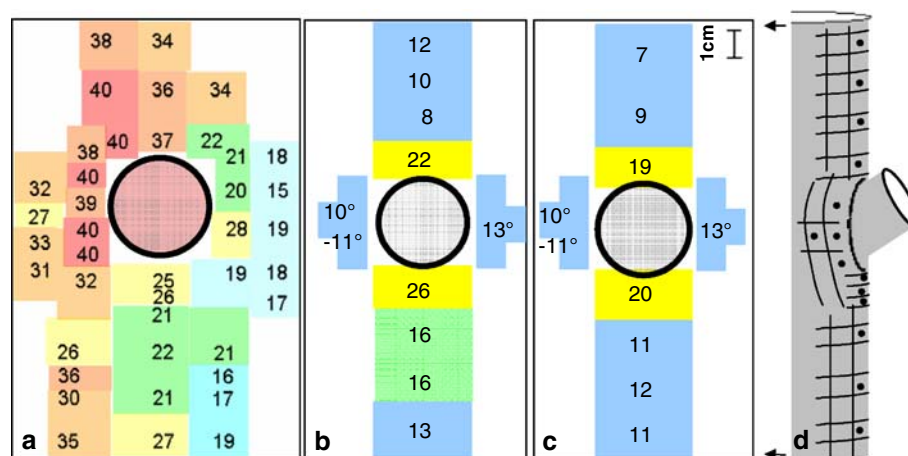
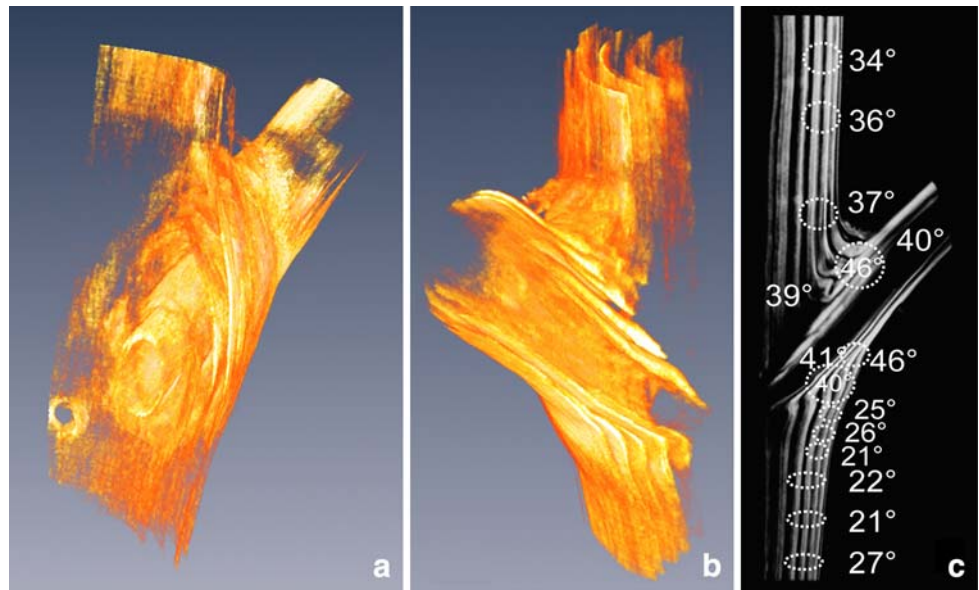


Fig. 3 Sketch of the MFA distribution around the branch junctions **a** ‘I’ **b** ‘II’ and **c** ‘III’ (flattened to 2D). **d** Schematic side view with sample positions of junction ‘II’ and ‘III’. The values are averages of the three outermost LW-MFA values at each position, values beside the branch in **b**, **c** are average values of two or three LW-layers

at four positions. In junction I, the MFA varied strongly between the growth rings, the average standard deviation was 4° (between 1.5 and 9°). For junction II and III, the average standard deviation was 2.3 and 2.9° . The region directly above and below the branch had the highest standard deviation (5 – 6°), the lowest (0.3°) was found at the left side

Fig. 4 CT of Junction I. Brightness corresponds to tissue density. Figure **b** is rotated to **a** and **c** by 180°. Layers of dense interface tissue and the lower density of the inner branch tissue are observable. **a** Shows the asymmetry of the density and thickness of LW to the left and the right side of the branch. The little ‘hole’ below the branch is due to a rudimentary twig. **b, c** Shows the distribution of density and MFA at the junction



stimulates diameter growth was e.g. made by Wilson and Archer (1979) and wind- or sway induced morphological adaptation of wood tissue was described by Telewski (1989). Increased MFA and density as response to (wind induced) tissue damage was described by Koch et al. (2000) and Trendelenburg (1940).

Junction I showed locally increased growth ring diameters beside the branch (increasing stem radius and stability) with increased LW density at the windward side (at the right side of the junction in Fig. 4b) and an overall increased MFA.

The CT showed that the density of the branch tissue at the base (and, as a consequence, also in the branch tissue included in the stem) was not as high as in the stem latewood. It also showed the increased density of the interface tissue inside the stem. Increased MFAs at the branch base were previously reported by Färber et al. (2001) and Burgert and Jungnickl (2004). In the present study, an increase of the MFA was observed in the included branch tissue as well as in the dense interface tissue (Fig. 4c). Tissue with high density and MFA provides high fracture toughness which is a desirable property at a junction, although it also provides some risk of severe stem injuries when the junction fails at the stem tissue (and not at the branch) and the toughness of the tissue does not allow a clean fracture but results in tearing of stem tissue below the branch and a large and rough fracture surface (Beismann et al. 2000). Tissue with low density and high MFA, as the branch base, provides deformability and flexibility. The combination of these two tissue types at the junction provides a mechanism to protect the stem against the transmission of forces and swaying moments from the branch, because a deformation

at the branch base will occur before forces are transmitted.

The high density of the interface tissue provides stiffness not only in the fibre direction (towards the branch) but also in the perpendicular direction, with the stem axis. A second function of the local increase of density could therefore be as a reinforcement to take up notch stresses from the axial forces in the stem.

Conclusion

We measured microfibril angle and density distribution at branch junctions of pines and found that the material properties vary locally as a response to the mechanical demands. This corresponds to an adaptation as was previously suggested by the homogeneous strain distribution in an ESPI experiment by Müller et al. (2006). High MFA values provide toughness in tissue with high density or flexibility in tissue with lower density. It was shown that MFA and density are adapted locally to provide regions of higher stiffness or flexibility, creating a pattern that is probably suited to protect the stem against notch stresses from axial tensile forces and against dynamic loads from the branch.

Acknowledgment Dietmar Meinel and Gerd Weidemann of the computer tomography group at the Federal Institute for Materials Research and Testing (BAM) are gratefully acknowledged for collecting the CT data.

Open Access This article is distributed under the terms of the Creative Commons Attribution Noncommercial License which permits any noncommercial use, distribution, and reproduction in any medium, provided the original author(s) and source are credited.

References

- Beismann H, Speck T, Bogenrieder A (1997) The wind in the willows—dispersal mechanisms and distribution of *Salix alba*, *S. fragilis* and their hybrid *S. rubens*. In: Jeronimidis G, Vincent JFV (eds) Plant biomechanics 1997. Conference proc. pp 57–64
- Beismann H, Wilhelmi H, Bailleres H, Spatz HC, Bogenrieder A, Speck T (2000) Brittleness of twig bases in the genus *Salix*: fracture mechanics and ecological relevance. *J Exp Bot* 51:617–633. doi:[10.1093/jexbot/51.344.617](https://doi.org/10.1093/jexbot/51.344.617)
- Böge A (2006) Technische Mechanik. Vieweg & Teubner Verlag, Wiesbaden
- Burgert I, Jungnikl K (2004) Adaptive growth of gymnosperm branches—ultrastructural and micromechanical examinations. *J Plant Growth Regul* 23:76–82. doi:[10.1007/s00344-004-0042-2](https://doi.org/10.1007/s00344-004-0042-2)
- Cave ID (1969) Longitudinal young's modulus of *Pinus radiata*. *Wood Sci Technol* 3:40–48. doi:[10.1007/BF00349983](https://doi.org/10.1007/BF00349983)
- Färber J, Lichtenegger HC, Reiterer A, Stanzl-Tschegg S, Fratzl P (2001) Cellulose microfibril angles in a spruce branch and mechanical implications. *J Mater Sci* 36:5087–5092. doi:[10.1023/A:1012465005607](https://doi.org/10.1023/A:1012465005607)
- Genenz V, Speck T, Bruechert F, Becker G (1997) Astbruch an Pappeln—biomechanische und morphogenetische Untersuchungen an *Populus x canadensis*. In: Dujesiefken D, Kockerbeck P (eds) Jahrbuch der Baumpflege 1997. Thalacker Medien, pp 204–209
- Koch G, Bauch J, Puls J, Schwab E (2000) Biological, chemical and mechanical characteristics of 'Wulstholz' as response to mechanical stress in living trees of *Picea abies* [L.] Karst. *Holzforschung* 54:137–143. doi:[10.1515/HF.2000.024](https://doi.org/10.1515/HF.2000.024)
- Lichtenegger H, Reiterer A, Tschegg S, Fratzl P (1998) Determination of spiral angles of elementary fibrils in the wood cell wall: comparison of small-angle x-ray scattering and wide-angle x-ray diffraction. In: Butterfield BGE (ed) Proceedings of the international workshop on the significance of microfibril angle to wood quality, Westport, 1997
- Mattheck C (1998) Design in nature. Springer, Berlin
- Müller U, Gindl W, Jeronimidis G (2006) Biomechanics of a branch-stem junction in softwood. *Trees (Berl)* 20:643–648. doi:[10.1007/s00468-006-0079-x](https://doi.org/10.1007/s00468-006-0079-x)
- Niklas KJ, Spatz HC (2000) Wind-induced stresses in cherry trees: evidence against the hypothesis of constant stress levels. *Trees (Berl)* 14:230–237. doi:[10.1007/s004680050008](https://doi.org/10.1007/s004680050008)
- Reiterer A, Lichtenegger H, Tschegg S, Fratzl P (1999) Experimental evidence for a mechanical function of the cellulose microfibril angle in wood cell walls. *Philos Mag A* 79:2173–2184
- Reiterer A, Lichtenegger H, Fratzl P, Stanzl-Tschegg SE (2001) Deformation and energy absorption of wood cell walls with different nanostructure under tensile loading. *J Mater Sci* 36:4681–4686. doi:[10.1023/A:1017906400924](https://doi.org/10.1023/A:1017906400924)
- Shigo AL (1989) A new tree biology. Shigo and Trees, Associates
- Telewski FW (1989) Structure and function of flexure wood in *Abies fraseri*. *Tree Physiol* 5:113–121
- Trendelenburg R (1940) Über Faserstauchungen in Holz und ihre Überwallung durch den Baum. *Holz Roh- und Werkst* 3:209–221
- Wilson BF, Archer RR (1979) Tree design—some biological solutions to mechanical problems. *Bioscience* 29:293–298. doi:[10.2307/1307825](https://doi.org/10.2307/1307825)